ELSEVIER

Carbohydrate Research 276 (1995) 365–386

CARBOHYDRATE RESEARCH

Structure of the *O*-deacetylated glucuronoxylomannan from *Cryptococcus neoformans* serotype C as determined by 2D ^{1}H NMR spectroscopy

Bradley E. Bacon, Robert Cherniak *

Department of Chemistry, Georgia State University, LBCS, Atlanta, GA 30303, USA

Received 1 February 1995; accepted 10 April 1995

Abstract

The primary structure of the *O*-deacetylated capsular glucuronoxylomannan (GXM) isolated from *Cryptococcus neoformans* serotype C was investigated by 2D NMR spectroscopy. Assignment of the ^{1}H NMR chemical shifts for the polysaccharide was accomplished from the analysis of DQF–COSY, TOCSY, NOESY and/or ROESY spectra of three isolates (298, 34, and 401). These isolates contain the same polysaccharide glycosyl residues but in different proportions. The serotype C GXM consists of two repeating polysaccharide units that have the following structures:

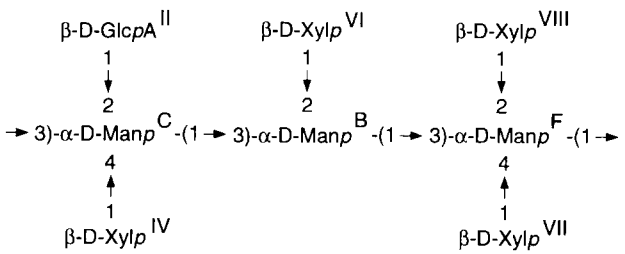

1

* Corresponding author.

Elsevier Science Ltd.
SSDI 0008-6215(95)00167-0

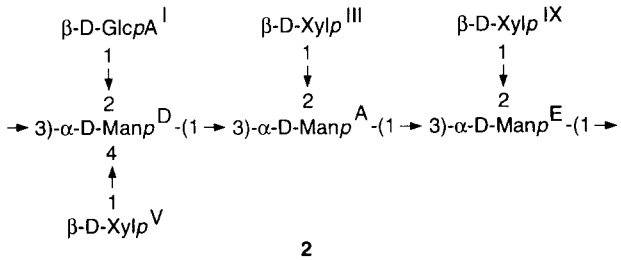

2

It is not known if these repeating units comprise a single or two separate polymer chains. The relative amounts of the more highly branched octasaccharide **1** in the isolates studied (i.e., approximately 75% in isolate 34, 50% in isolate 298, and 25% in isolate 401) can be used to explain the serological specificity of these isolates with *C. neoformans* factor sera, as was previously determined by ELISA in this laboratory. The octasaccharide **1** component is the one previously postulated as the structure of the serotype C GXM although definitive placement of the β-Xyl-(1 → 4) residues had previously not been determined. The heptasaccharide **2** component is uniformly found as the repeating unit in the polysaccharide from serotype B isolates. Additionally, GXM 401 was found to contain a small amount of the hexasaccharide repeating unit usually attributed to serotype A GXM.

Keywords: *Cryptococcus neoformans*; 2D NMR spectroscopy; Capsular polysaccharide

1. Introduction

Cryptococcus neoformans is an encapsulated yeast responsible for meningoencephalitis in individuals with suppressed immune systems [1]. Up to 10% of patients diagnosed with AIDS are also suffering from cryptococcosis [2,3]. The yeast's virulence is partially due to its polysaccharide capsule. The properties of the capsular polysaccharide antigenic components have recently been reviewed [4]. The major capsular antigen is a high molecular weight glucuronoxylomannan (GXM) that is partially 6-*O*-acetylated on mannose [5–7]. Serological reactivity of the capsular polysaccharide has traditionally been used to define four serotypes (A, B, C, and D) [8,9] that have been classified into two varieties based on biochemical differences: var. *neoformans* (serotypes A and D) and var. *gattii* (serotypes B and C) [10–12]. The existence of a fifth serotype, A-D, has been described more recently [13]. Most cryptococcal infections in AIDS patients are due to *C. neoformans* var. *neoformans* [14], although a few cases of cryptococcosis due to *C. neoformans* var. *gattii* have been reported [15–19]. The *gattii* variety has been associated with more severe infections in humans [20].

A simple structural relationship between the GXM polysaccharides of the four serotypes exists. They are composed of a core repeating unit,

β-D-Glc*p*A
1
↑
2
→ 3)-α-D-Man*p*-(1 → 3)-α-D-Man*p*-(1 → 3)-α-D-Man*p*-(1 →

to which (1 → 2)-linked β-D-Xyl*p* and (1 → 4)-linked β-D-Xyl*p* residues are added to the (1 → 3)-linked α-D-mannopyrannan backbone. Homogeneous structural models were originally proposed for the four serotypes based on precise molar Xyl/Man/GlcA ratios of 1:3:1, 2:3:1, 3:3:1, and 4:3:1 for serotypes D, A, B, and C, respectively, with Xyl*p* substitution at O-2 for the var. *neoformans* serotypes and Xyl*p* substitution at O-2 and O-4 for the var. *gattii* serotypes [5]. Structural heterogeneity has since been found for all serotypes except serotype B [21], and structural elements believed to be characteristic of one serotype have been identified in others [7,22–24].

The original structural model of serotype C GXM was proposed on the basis of gas–liquid chromatography–mass spectrometric (GLC–MS) analysis of per-*O*-methylated sugar derivatives of GXM from a single serotype C isolate [25,26]. Cherniak et al. later detected heterogeneity within serotype C isolates, which were classified into two groups based on the molar Xyl/Man/GlcA ratios determined for five isolates [23]. Three isolates (GXMs 401, 3183, and 18) were found to have molar Xyl/Man/GlcA ratios similar to those for serotype B isolates (3:3:1); the other two isolates (GXMs 298 and 34) were found to contain additional Xyl, but not enough to account for a 4:3:1 Xyl/Man/GlcA molar ratio. Whereas the proton-decoupled ^{13}C NMR spectra of GXMs from strains 18 and 3183 resembled the spectra from GXMs of serotype B isolates, the spectra of isolates 401, 298, and 34 were different enough from each other, as well as from serotype B isolates, to warrant further analysis. The activities of these same isolates with factor serum specific for *C. neoformans* serotype C GXM have recently been found to increase progressively in the order 18, 3183, 401, 298, and 34, as determined by enzyme-linked immunosorbent assay (ELISA) [27].

The *O*-deacetylated GXMs from serotype D [28], B [29], and A [30] isolates have previously been characterized by 2D NMR spectroscopy. Herein we report the complete assignment of the ^{1}H NMR spectra of *O*-deacetylated GXM from three *C. neoformans* serotype C isolates (298, 34, and 401) as determined by 2D NMR spectroscopy [31].

2. Experimental

GXM polysaccharides.—The isolation and purification of the *O*-deacetylated GXMs used in this study have previously been described [23]. GXM polysaccharides from the following isolates were used: National Institutes of Health isolates 298, 34, and 401, serotype C (K.J. Kwon-Chung, National Institutes of Health).

Nuclear magnetic resonance spectroscopy.—Spectra were recorded with a Varian VXR-400 NMR spectrometer equipped with a 5 mm $^{1}H/^{19}F$ probe and operating at 399.952 MHz for ^{1}H observation. The observed ^{1}H chemical shifts are reported relative to HOD, which was carefully calibrated according to temperature with internal sodium 4,4-dimethyl-4-silapentane-1-sulfonate (DSS). All spectra for GXM 298 and GXM 34 were recorded at 69 and 68°C, respectively. Spectra for GXM 401 were recorded at 68°C unless otherwise noted. Resolution enhancement of one-dimensional spectra was performed using a shifted sine-bell squared.

Polysaccharide samples (20–30 mg) were exchanged at least 2 times in 99.96% D_2O with intermediate lyophilization. The NMR samples were prepared by final dissolution in 0.750 mL of 99.96% D_2O.

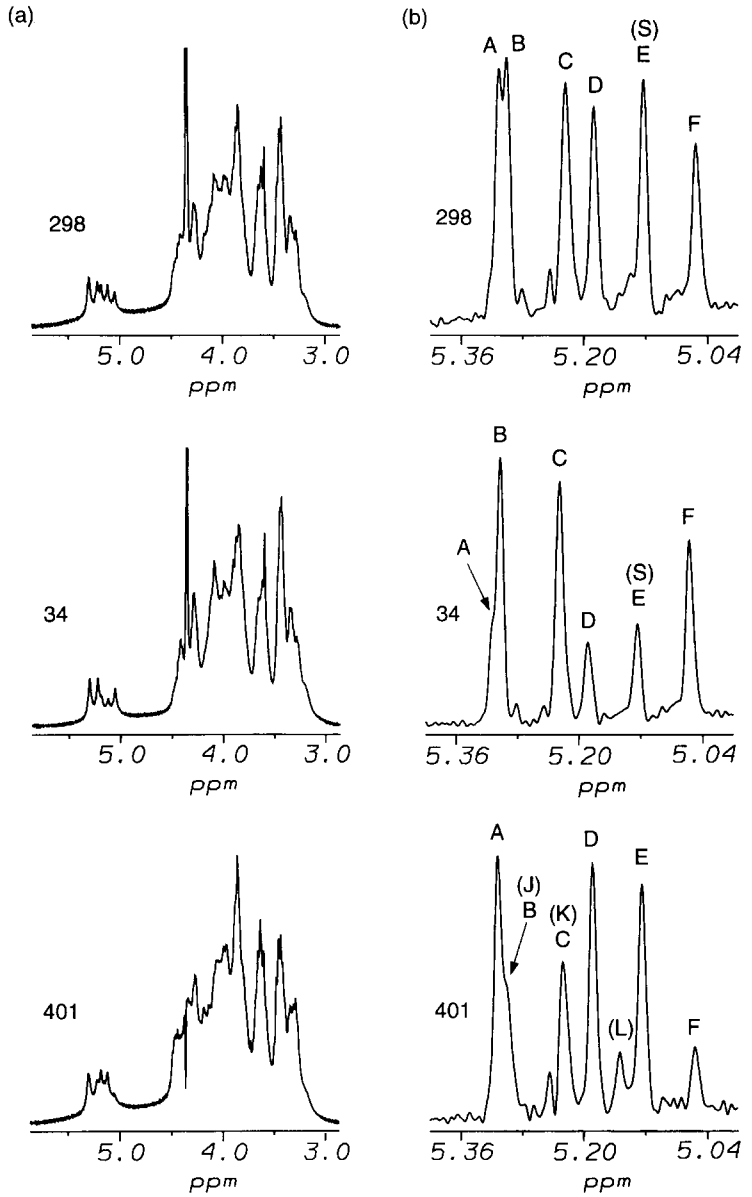

Fig. 1. (a) 400-MHz ^{1}H NMR spectra of *O*-deacetylated GXM from serotype C isolates 298, 34, and 401 (top, middle, and bottom, respectively). (b) Resolution-enhanced portions of the 5.4–5.0 ppm regions shown in (a). The major H-1 resonances of GXM 298 in this region are labeled with upper-case letters A, B, C, D, E, and F and refer to different Man residues present in all three isolates. Minor H-1 resonances are indicated by upper-case letters enclosed in parentheses and indicate minor amounts of Man residues not common to all three isolates.

All 2D NMR spectra were acquired in the phase-sensitive mode according to the method of States et al. [32]. The spectral width was 1200 Hz in both dimensions, and two sets of 175–256 t_1 measurements of 2048 data points were acquired. Zero filling in the $F1$ dimension resulted in a 1K × 1K data matrix.

Double-quantum-filtered $^1H-^1H$ correlation spectroscopy (DQF–COSY) was carried out according to refs [33] and [34]. Resolution enhancement in the $F2$ dimension was achieved using the product of a −8 Hz Gaussian transformation and a −6 Hz exponential multiplication (GXMs 298 and 34) or a −8 Hz Gaussian transformation (GXM 401). Resolution enhancement in the $F1$ dimension was achieved using a shifted sine-bell (GXMs 298 and 34: 22.5°, GXM 401: 45°).

Homonuclear Hartmann–Hahn (HOHAHA or TOCSY—total correlation spectroscopy) spectra were obtained for isolates 298 and 34 (mixing times 50 and 100 ms) and for isolate 401 (mixing time 100 ms) according to ref. [35]. Spectra were multiplied by a 90° shifted sine-bell squared and by a 45° shifted sine-bell in the $F2$ and $F1$ dimensions, respectively.

Nuclear Overhauser and exchange spectroscopy (NOESY) was carried out on all three isolates according to ref. [36] (mixing time 50 ms). Resolution enhancement was achieved using a shifted sine-bell squared in both dimensions.

Rotating frame Overhauser spectroscopy (ROESY) [37,38] was carried out for GXMs 34 and 401 (71°C) according to ref. [39]. A cosine squared and 45° shifted sine-bell were used as apodization for the $F2$ and $F1$ dimensions, respectively. The ROESY spectra were recorded with a 75 ms mixing time.

A purged COSY (P.COSY) experiment [40] was performed for GXM 401 at 71°C. Resolution enhancement was achieved using a −8 Hz Gaussian function and a 45° shifted sine-bell in the $F2$ and $F1$ dimensions, respectively.

3. Results

The one-dimensional ^1H NMR spectra of the *O*-deacetylated capsular polysaccharide of serotype C isolates 298, 34, and 401 show broad, unresolved signals even at elevated temperatures (Fig. 1a). With the use of strong resolution enhancement, six major signals of about the same intensity are observed for isolate 298 in the downfield anomeric region (Fig. 1b: A, B, C, D, E, and F at 5.31, 5.30, 5.22, 5.19, 5.12, and 5.05 ppm, respectively). These signals are also present in the spectrum of isolates 34 and 401: three of these signals (B, C, and F) are of greater intensity in the spectrum of isolate 34 while the other three signals (A, D, and E) are of greater intensity in the spectrum of isolate 401; isolate 401 has at least one additional prominent minor signal at 5.15 ppm, L (Fig. 1b). Resonances A–F are assigned to Man H-1 protons since weak H-1–H-2 cross peaks ($^3J_{1,2} < 4$ Hz) are observed in the DQF–COSY spectra (portions of which are shown in Figs 2 and 3 for isolates 401 and 34, respectively). No propagation of magnetization transfer beyond H-2 is observed due to the small value of $^3J_{1,2}$ [28], and TOCSY correlations to only H-2 are observed (data not shown). Previous structural analysis of these isolates by ^{13}C NMR spectroscopy had failed to show the presence of the corresponding Man anomeric carbon signals, due mainly to a lack of resolved signals for

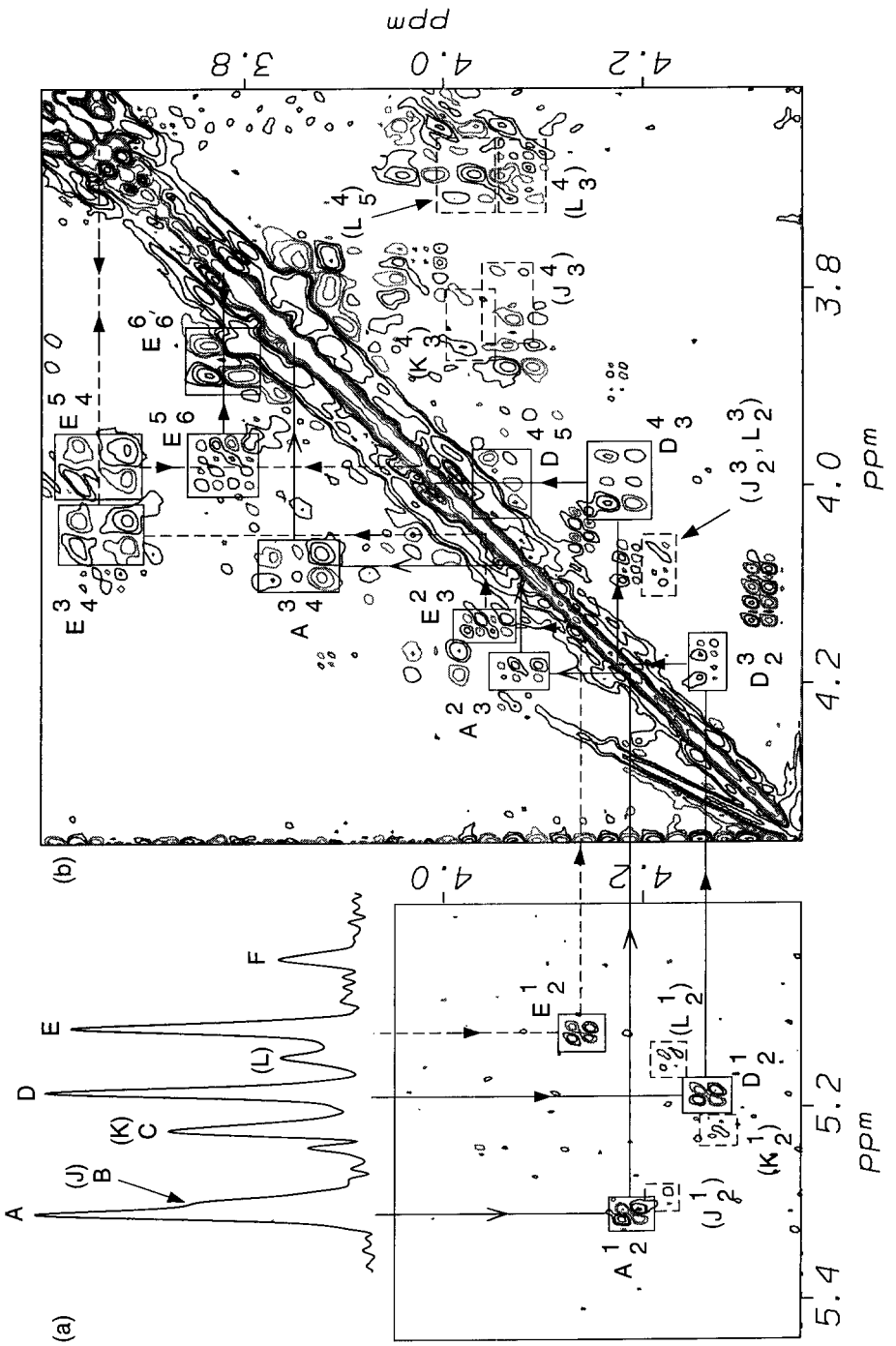
(a)
(b)
A
(J) B
C
(K)
D
(L)
E
F
ppm
5.4
5.2
4.2
4.0
3.8

isolate 34. Serotype 401 had been found to consist primarily of a carbohydrate structure similar to that of serotype B [23].

The individual monomers of a carbohydrate polymer are identified by tracing cross-peak connectivities between vicinally coupled protons in a phase-sensitive DQF–COSY spectrum. The downfield anomeric Man proton region shown in Fig. 1b provides a convenient starting point for tracing these connectivities. Starting from the major A, D, and E H-1 resonances for GXM 401, the connectivities for residues Man-A, Man-D, and Man-E are traced from H-1 to H-4 via their respective H-1–H-2, H-2–H-3, and H-3–H-4 cross peaks (Fig. 2). Man-D is traced further to H-5 via its H-4–H-5 cross peak while Man-E is traced to H-6 through to its H-5–H-6 and H-6–H-6′ cross peaks.

The analogous cross-peak connectivity tracings for the major B, C, and F H-1 resonances for GXM 34 are shown in Fig. 3. Man-C is traced from H-1 to H-4, while Man-F is traced from H-1 to H-6 with its H-2–H-3 cross peak only partially discernible close to the diagonal. Connectivity from H-1 to H-4 was made for Man-B in spite of the fact that its H-2–H-3 cross peak is totally obscured by the diagonal; the Man-B H-3–H-4 cross peak was assigned as such because H-3–H-4 cross peaks had already been assigned for the Man-C and Man-F residues. Although positive and negative peaks are not clearly discernible in Figs 2 and 3, the phase-sensitive nature of the DQF–COSY experiment allows the qualitative measurement of coupling constants, consistent with assignment to a Man$p$ $^4C_1$ conformation for residues A, B, C, D, E, and F ($^3J_{1,2} < 4$ Hz, $^3J_{2,3} < 4$ Hz, $^3J_{3,4} > 5$ Hz, $^3J_{4,5} > 5$ Hz).

H-6–H-6′ cross peaks for residues B and C are labeled in Fig. 3, despite the fact that they show no connectivity to other cross peaks. These cross peaks were assigned with the use of TOCSY spectra of GXM 34 recorded with mixing times of 50 ms and 100 ms; portions of these spectra are shown in Fig. 4. As we have observed for several other GXM isolates, the 50 ms TOCSY spectrum in Fig. 4a is useful for assigning Man H-5 protons from the observed H-3–H-5 relay peaks [41]. The 100 ms TOCSY spectrum in Fig. 4b shows a H-3–H-6 relay peak for residue C; this cross peak also appears in Fig. 4a, where it partially overlaps the Man-C H-3–H-5 cross peak. A cross peak for Man-C H-6–H-6′ is also labeled in Fig. 4b and corresponds to the DQF–COSY cross peak labeled in Fig. 3. It is important to note that H-4, H-5, and H-6 of Man-C have similar

Fig. 2. (a) Mannose H-1–H-2 cross peak region of the phase-sensitive DQF–COSY spectrum of *O*-deacetylated GXM 401 recorded at 400 MHz and 68°C, with resolution-enhanced 1D projection at top. (b) The 4.3–3.6 ppm region of the DQF–COSY spectrum shown in (a). This region contains resonances for Man H-2, H-3, H-4, H-5, H-6, and H-6′ protons. Positive and negative levels of cross peaks are shown in different line styles. Arabic numerals denote proton positions in the given residue (specified by upper-case letters as in Fig. 1). In a cross peak label, the superscript denotes the proton whose chemical shift is given on the $F2$ (horizontal scale) axis, and the subscript denotes the proton whose chemical shift is given on the $F1$ (vertical scale) axis. The lines trace the connectivities for Man residues A, D, and E; cross peaks for these residues are boxed with solid lines. Each line begins at the appropriate H-1 resonance in (a), goes down to the H-1–H-2 cross peak, on to the diagonal in (b), and on to the next cross peak. It continues in this manner until the connectivity is traced for each residue. To avoid crowding in (b), the cross peaks for Man residues A and E are labeled above the diagonal, and cross peaks for Man residue D are labeled below the diagonal. The cross peaks for Man residues J, K, and L are boxed with dotted lines below the diagonal, and the labels for these cross peaks are presented in parentheses.

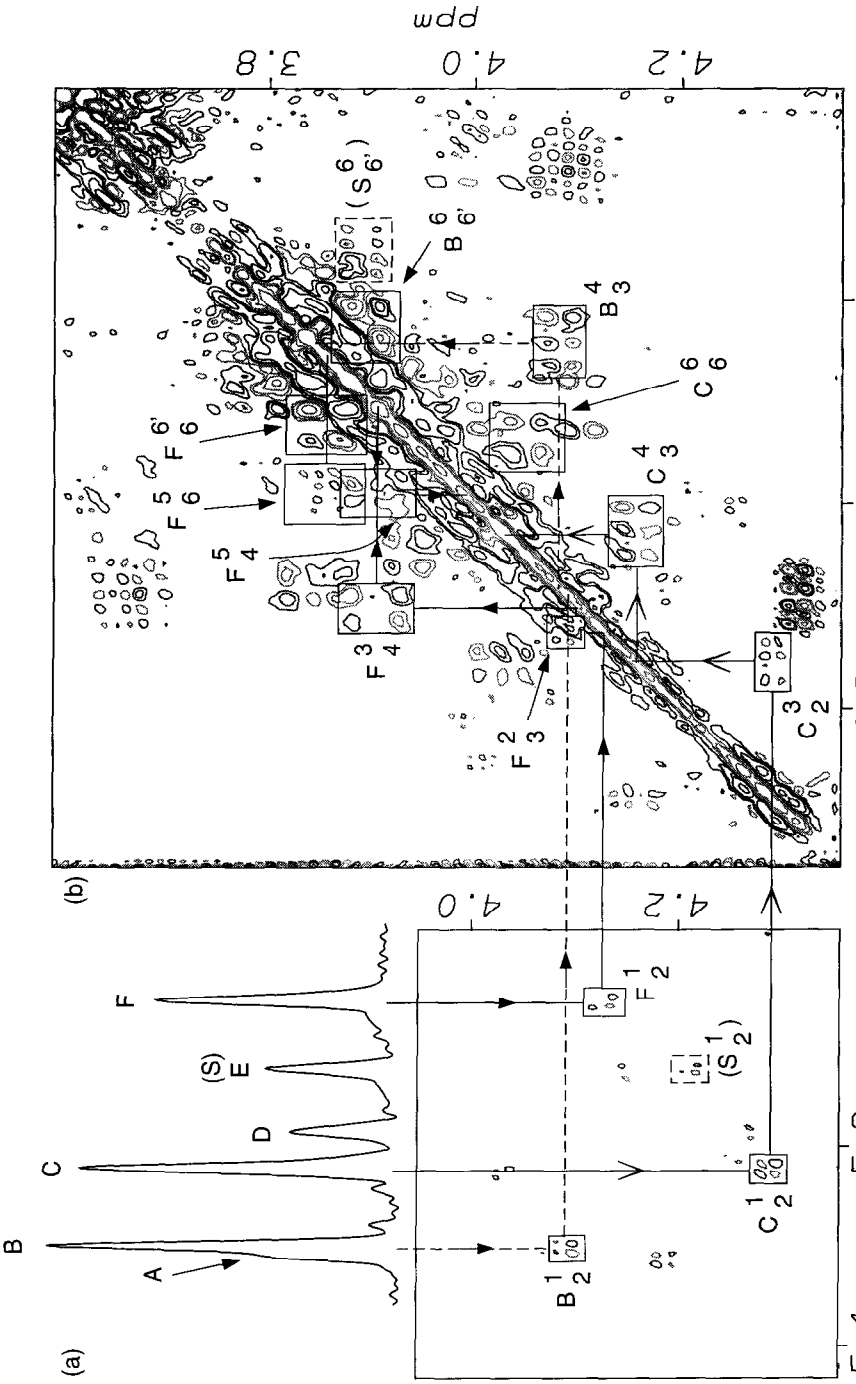

Fig. 3. (a) Mannose H-1–H-2 cross peak region of the phase-sensitive DQF–COSY spectrum of *O*-deacetylated GXM 34 recorded at 400 MHz and 68°C, with resolution-enhanced 1D projection at top. (b) The 4.3–3.6 ppm region of the DQF–COSY spectrum shown in (a). This region contains resonances for Man H-2, H-3, H-4, H-5, H-6, and H-6′ protons. Positive and negative levels of cross peaks are shown in different line styles. Cross peaks are marked in the manner described in Fig. 2. Cross peak connectivities for Man residues B, C, and F are traced as in Fig. 2. To avoid crowding in (b), the cross peaks for Man-F are labeled above the diagonal, and the cross peaks for Man-B and Man-C are labeled below the diagonal; all cross peaks for these residues are enclosed in solid lined boxes. Cross peaks for Man-S are boxed with dotted lines and are labeled within parentheses.

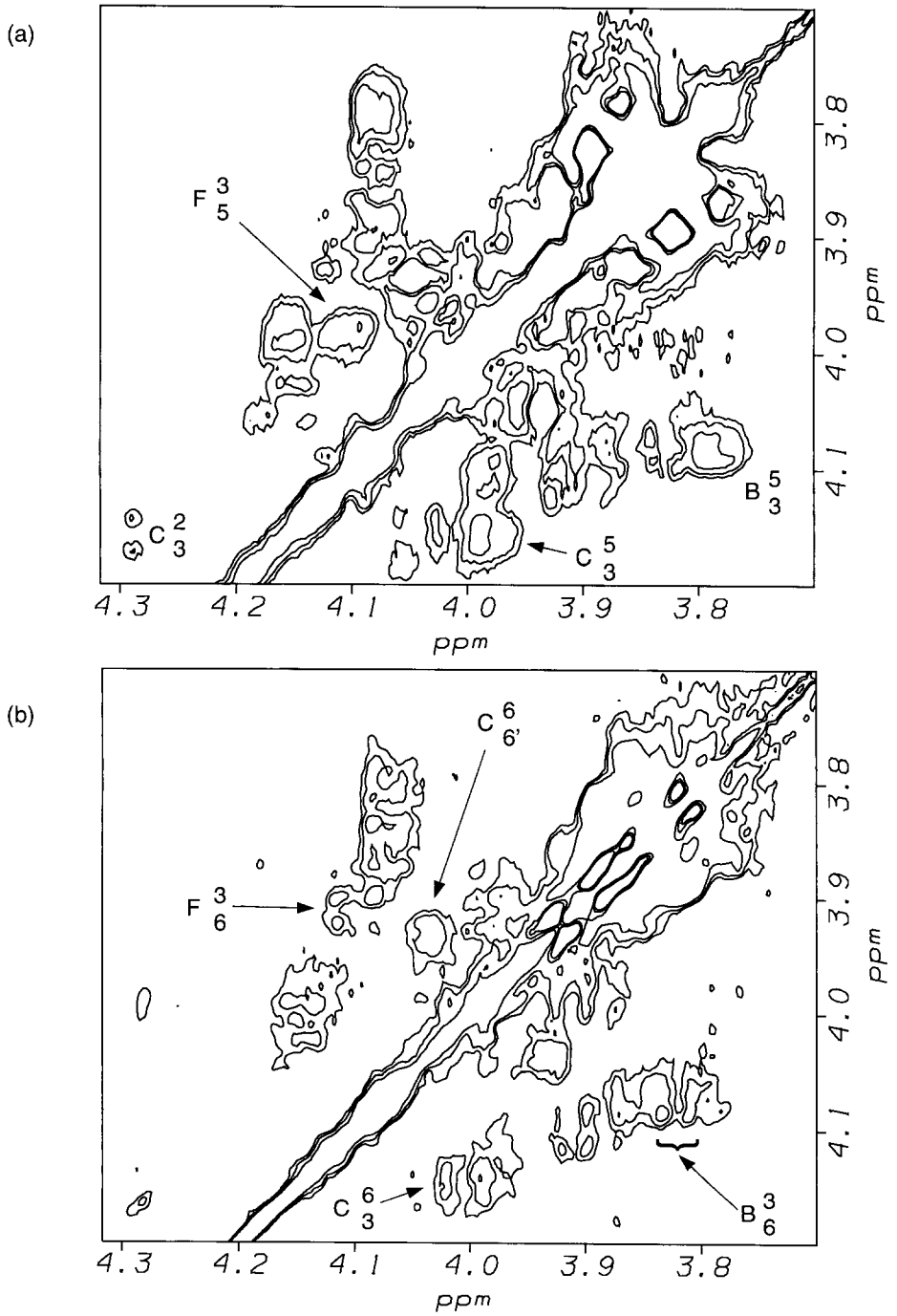

Fig. 4. (a) Portion of the 50 ms TOCSY spectrum of GXM 34, and (b) the corresponding portion of the 100 ms TOCSY spectrum of GXM 34. The labeling for cross peaks is the same as for Fig. 2.

chemical shifts; consequently, non-first-order coupling is involved. Hence, the cross peak that is most certainly due to active coupling between Man-C H-6 and H-6′ is not centered around the actual H-6 chemical shift, as measured from the Man-C H-3–H-6 relay peak in Fig. 4b. The cross peak labeled Man-B H-6–H-6′ in Fig. 3 was assigned mainly because the H-6–H-6′ cross peaks for residues C and F had already been identified. However, a corresponding Man-B H-3–H-6 relay peak (marked in Fig. 4b), overlaps with what is certainly the Man-B H-3–H-4 cross peak.

Tracing the cross-peak connectivities of Man residues of the *O*-deacetylated GXM of isolate 298 was performed in a similar manner; the presence of some overlapping cross peaks (particularly those H-3–H-4 cross peaks of residues A and B) necessitated reference to chemical shift assignments already deduced from isolates 34 and 401. Most of the Man cross peaks for GXM 298 are labeled in Fig. 5, which shows the entire DQF–COSY spectrum of GXM 298 except for the Man H-1–H-2 cross peak region. Small traces of cross peaks due to other Man residues in addition to those marked for residues A–F are apparent in Fig. 5; however, only the Man-S H-2–H-3 cross peak is labeled. This additional Man residue is the only one present in sufficient quantity to be observed by NOESY and/or ROESY experiments. The Man-S residue is also present in GXM 34; Man-S H-1–H-2 and H-6–H-6′ cross peaks are identified in Fig. 3. Complete assignments of protons belonging to the Man-S residue were made using appropriate contour levels of the DQF–COSY spectra of isolates 298 and 34. Complete chemical shift assignments of Man resonances for the *O*-deacetylated GXM of isolates 298, 34, and 401 are presented in Table 1. TOCSY spectra of isolates 298 and 401 were used to assign certain Man H-5, H-6, and H-6′ chemical shifts as described above for GXM 34. The chemical shifts for the major Man residues of GXM 401 closely match those reported for the *O*-deacetylated GXM of serotype B [29].

The DQF–COSY spectrum shown above the diagonal in Fig. 5a shows nine distinct H-1–H-2 cross peaks (labeled for GlcA residues: GlcA-I and GlcA-II, and for Xyl residues: III, IV, V, VI, VII, VIII, and IX), which are consistent with assignment to a β-D-Xyl*p* or to a β-D-Glc*p*A structure ($^3J_{1,2} > 6$ Hz, $^3J_{2,3} > 6$ Hz). One of these H-1–H-2 cross peaks (VII) shows distorted multiplicity indicative of strong coupling between H-2 and H-3. The cross peaks for residues VIII and IX overlap. Complete cross peak connectivities between protons in these nine carbohydrate residues are difficult to observe since, aside from the H-1–H-2 cross peaks, the other cross peaks for these ring systems overlap with other cross peaks or diagonal peaks. Nevertheless, many of the corresponding H-2–H-3 and H-3–H-4 cross peaks were identified by close examination of expanded contour plots of the 3.7–3.2 ppm region. The chemical shifts of the Xyl and GlcA residue H-3 and H-4 protons can also be roughly obtained from the H-1–H-3 and H-1–H-4 relay peaks shown in the boxed region of the TOCSY spectrum in Fig. 5b. Approximate ranges for location along the *F*2 (or horizontal) axis of these relay peaks are marked above the box with the chemical shift along this axis being due to H-4, H-3, or H-2 in the three ranges marked. The assignment of any residue as a GlcA or a Xyl residue cannot be made using the DQF–COSY spectrum of isolate 298 since no H-4–H-5 GlcA cross peaks are clearly resolved from the diagonal and since Xyl H-4–H-5a, H-4–H-5e, and H-5a–H-5e cross peaks are poorly identified due to extensive overlap and partial cancellation. However, from the examination of cross sections

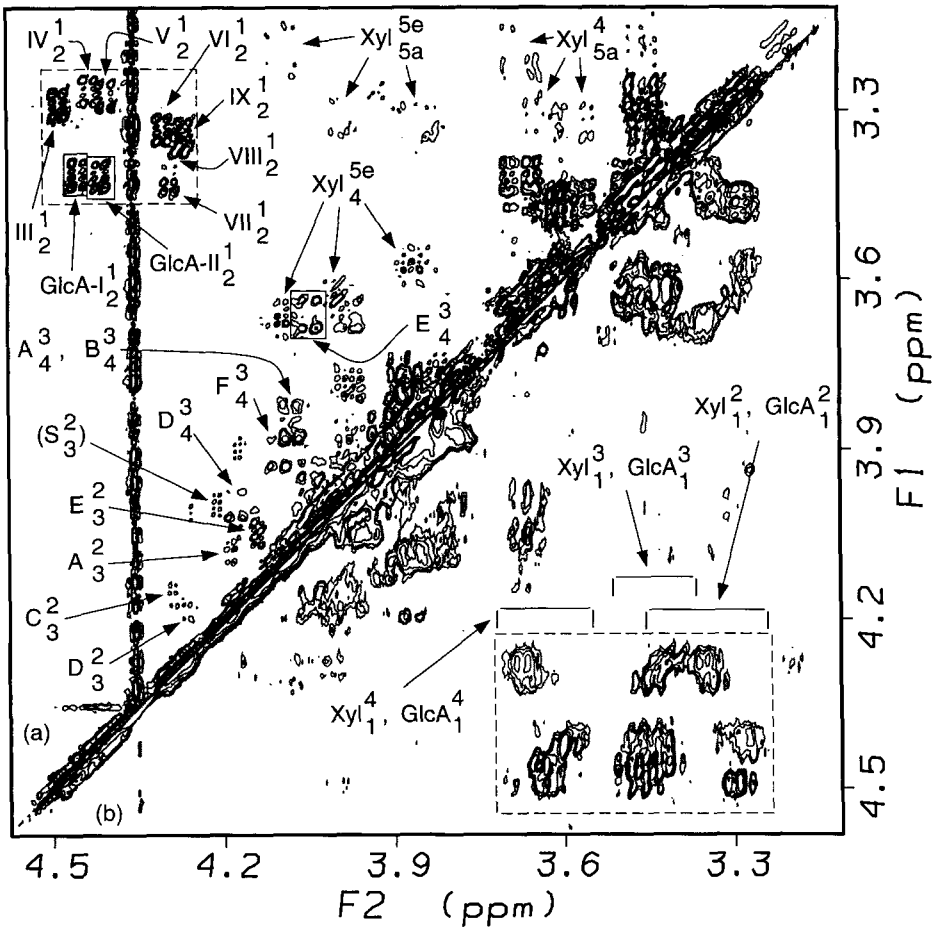

Fig. 5. (a) Portion of the phase-sensitive DQF–COSY spectrum of *O*-deacetylated GXM 298 recorded at 400 MHz and 69°C (above the diagonal); only the Man H-1 region (H-1–H-2 cross peaks) is excluded. Roman numerals refer to Xyl and GlcA residues; the GlcA residues are marked explicitly as, for example, GlcA-II. Otherwise, cross peaks are labeled as described for Figs 2 and 3. (b) The corresponding part of the phase-sensitive 100 ms TOCSY spectrum of GXM 298 (below the diagonal). The boxed region shows Xyl and GlcA H-1–H-2, H-1–H-3, and H-1–H-4 cross peaks; the ranges of chemical shifts covered for each of these peaks along the *F*2 (horizontal) axis are marked.

of the TOCSY spectrum through the *F*1 chemical shifts of GlcA-I and GlcA-II, these two residues were thought to be GlcA residues as a result of observing H-1–H-5 relay peaks that overlap with the respective H-1–H-4 relay peaks. Approximate locations of the Xyl DQF–COSY cross peaks (H-4–H-5a, H-4–H-5e, and H-5a–H-5e) are marked in Fig. 5a.

Just as the DQF–COSY spectra of GXM 34 and GXM 401 were useful in discriminating between overlapping Man-A H-3–H-4 and Man-B H-3–H-4 cross peaks in the DQF–COSY spectrum of GXM 298, the DQF–COSY spectra were especially

Table 1
^{1}H NMR chemical shifts of the ring protons of the constituent mannose residues of **1**, **2**, and **5** as identified in the *O*-deacetylated GXM of *C. neoformans* serotype C isolates 298, 34, and 401

		Chemical shift [a]						
	Isolate	Man-A [b]	Man-B	Man-C	Man-D	Man-E	Man-F	Man-S
H-1	298	5.311 [c]	5.299	5.224	5.188	5.124	5.054	5.121
	34 [d]	n.d. [e]	5.300	5.222	n.d.	n.d.	5.056	5.121
	401 [f]	5.311	n.d.	n.d.	5.188	5.124	n.d.	– [g]
H-2	298	4.188	4.090	4.290	4.266	4.140	4.128	4.212
	34	n.d.	4.091	4.289	n.d.	n.d.	4.126	4.211
	401	4.189	n.d.	n.d.	4.264	4.139	n.d.	–
H-3	298	4.079	4.080	4.157	4.178	4.047	4.102	3.996
	34	n.d.	4.083	4.155	n.d.	n.d.	4.104	3.997
	401	4.079	n.d.	n.d.	4.178	4.046	n.d.	–
H-4	298	3.856	3.842	4.028	3.995	3.661	3.904	3.774
	34	n.d.	3.842	4.028	n.d.	n.d.	3.904	3.775
	401	3.855	n.d.	n.d.	3.994	3.660	n.d.	–
H-5	298	3.87 [h]	3.80 [h]	3.99 [h]	4.06 [h]	3.978	3.985	3.831
	34	n.d.	3.79 [h]	3.98 [h]	n.d.	n.d.	3.990	3.831
	401	3.87 [h]	n.d.	n.d.	4.054	3.977	n.d.	–
H-6	298	n.a. [i]	n.a.	n.a.	n.a.	3.784	n.a.	3.754
	34	n.d.	3.896	4.013	n.d.	n.d.	3.857	3.754
	401	3.84	n.d.	n.d.	3.96	3.783	n.d.	–
H-6′	298	n.a.	n.a.	n.a.	n.a.	3.873	n.a.	3.890
	34	n.d.	3.825	3.94	n.d.	n.d.	3.924	3.894
	401	n.a.	n.d.	n.d.	n.a.	3.872	n.d.	–

[a] In ppm relative to HOD as externally referenced according to temperature with DSS (δ 0.0) as internal standard.
[b] For residue labeling see formulae.
[c] Unless otherwise noted, chemical shifts were assigned from a DQF–COSY spectrum of the respective GXM isolate recorded at 69°C (GXM 298) or 68°C (GXM 34 and GXM 401) and are reported to three decimal places with an accuracy of ± 0.003 ppm. Shifts given to two decimal places were deduced from TOCSY, NOESY, or ROESY spectra.
[d] Chemical shifts for minor amounts of residues A, D, and E in GXM 34 not determined.
[e] Not determined.
[f] Chemical shifts for minor amounts of residues B, C, and F in GXM 401 not determined.
[g] Not applicable.
[h] Assigned from 50 ms NOESY spectrum of respective isolate (from interresidue H-2–H-5 cross peak).
[i] Not assigned.

useful in discriminating Xyl and GlcA cross peaks linked either to the major B, C, and F Man residues of isolate 34 or to the major A, D, and E Man residues in isolate 401. Nearly complete assignments of ring protons belonging to GlcA residue GlcA-II and to Xyl residues IV, VI, VII, and VIII were obtained from the DQF–COSY spectrum of isolate 34, assignments of those protons belonging to residues GlcA-I, III, V, and IX were obtained from the DQF–COSY spectrum of isolate 401. At suitable contour levels, the Xyl H-4–H-5e, and H-5a–H-5e cross peaks were identifiable for Xyl residues III, IV, V, VI, VII, VIII, and IX (in contrast to the situation for isolate 298); this is shown for residues IV, VI, VII, and VIII in Fig. 6b, which shows a portion of the DQF–COSY

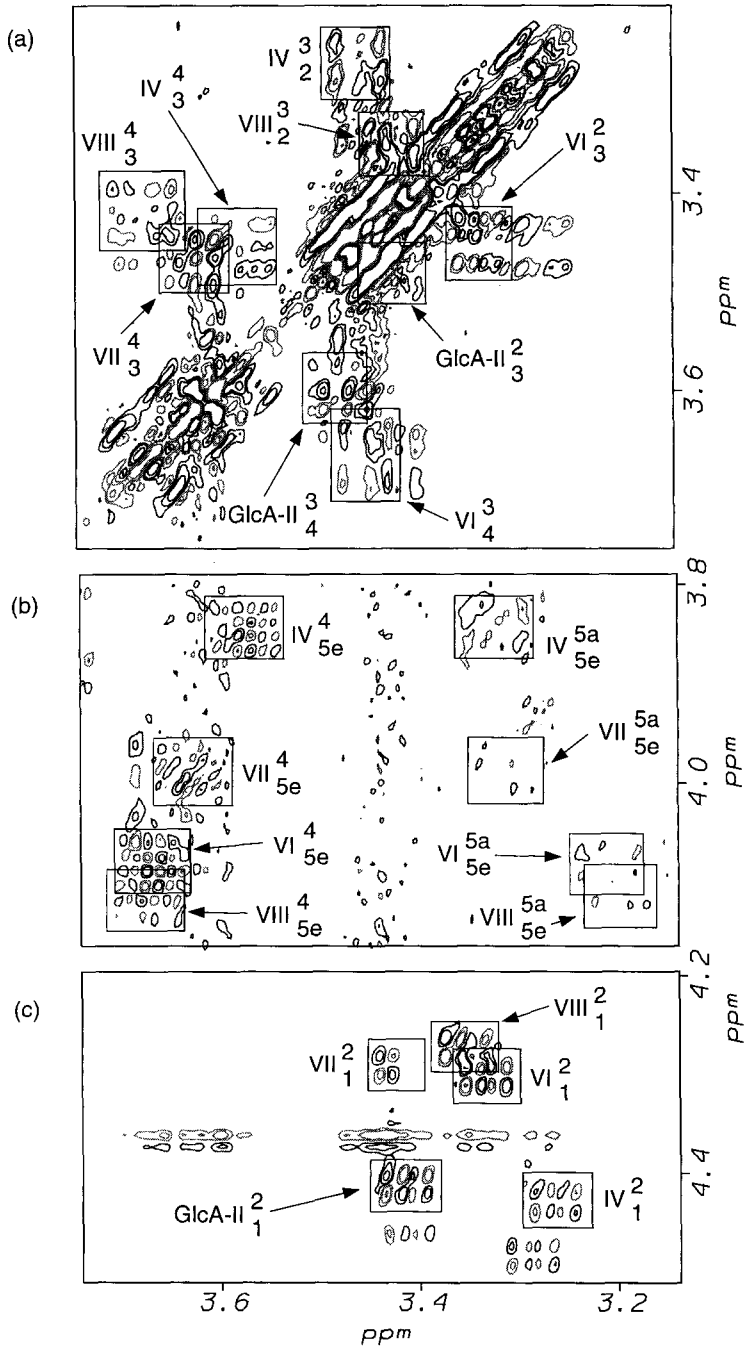

Fig. 6. Portions of the DQF–COSY spectrum of *O*-deacetylated GXM 34. These regions contain cross peaks for the Xyl and GlcA residues (IV, VI, VII, and VIII, and GlcA-II) which are linked to the major Man residues of GXM 34 (B, C, and F). The middle region containing H-1–H-5e and H-5a–H-5e cross peaks (b) is at a lower contour level than the top and bottom regions ((a) [H-2–H-3 and H-3–H-4 cross peaks] and (c) [H-1–H-2 cross peaks], respectively). Cross peaks are labeled as in Figs 2, 3, and 5.

Table 2
^{1}H NMR chemical shifts of the ring protons of the constituent xylose and glucuronic acid residues of **1** and **2** as identified in the *O*-deacetylated GXM of *C. neoformans* serotype C isolates 298, 34, and 401

		Chemical shift [a]								
	Isolate	GlcA-I [b]	GlcA-II	Xyl-III	Xyl-IV	Xyl-V	Xyl-VI	Xyl-VII	Xyl-VIII	Xyl-IX
H-1	298	4.452 [c]	4.412	4.484	4.430	4.401	4.302	4.291	4.272	4.266
	34 [d]	n.d. [e]	4.412	n.d.	4.431	n.d.	4.302	4.292	4.273	n.d.
	401 [f]	4.452	n.d.	4.483	n.d.	4.400	n.d.	n.d.	n.d.	n.d.
H-2	298	3.412	3.416	3.290	3.266	3.274	3.334	3.422	3.354	3.342
	34	n.d.	3.415	n.d.	3.266	n.d.	3.334	3.422	3.356	n.d.
	401	3.412	n.d.	3.288	n.d.	3.274	n.d.	n.d.	n.d.	3.342
H-3	298	3.482	n.a. [g]	3.457	3.457	3.459	3.450	3.470	3.424	3.415
	34	n.d.	3.482	n.d.	3.456	n.d.	3.450	3.470	3.422	n.d.
	401	3.481	n.d.	3.456	n.d.	3.459	n.d.	n.d.	n.d.	3.414
H-4	298	3.598	3.598	3.632	n.a.	n.a.	3.666	3.623	3.674	3.674
	34	n.d.	3.598	n.d.	3.577	n.d.	3.666	3.624	3.674	n.d.
	401	3.598	n.d.	3.632	n.d.	3.577	n.d.	n.d.	n.d.	3.672
H-5a	298	3.630 [h]	3.600 [h]	n.a.	n.a.	n.a.	n.a.	n.a.	n.a.	n.a.
	34	n.d.	3.599 [h]	n.d.	3.322	n.d.	3.211	3.313	3.198	n.d.
	401	3.632 [h]	n.d.	3.313	n.d.	3.324	n.d.	n.d.	n.d.	3.181
H-5e	298	– [i]	–	n.a.	n.a.	n.a.	n.a.	n.a.	n.a.	n.a.
	34	–	–	n.d.	3.846	n.d.	4.081	4.001	4.110	n.d.
	401	–	–	3.994	n.d.	3.873	n.d.	n.d.	n.d.	4.080

[a] In ppm relative to HOD as externally referenced according to temperature with DSS (δ 0.0) as internal standard.
[b] For residue labeling see formulae.
[c] Unless otherwise noted, chemical shifts were assigned from a DQF–COSY spectrum of the respective GXM isolate recorded at 69°C (GXM 298) or 68°C (GXM 34 and GXM 401) and are reported to three decimal places with an accuracy of ± 0.003 ppm.
[d] Chemical shifts for minor amounts of residues GlcA-I, III, V, and IX in GXM 34 not determined.
[e] Not determined.
[f] Chemical shifts for minor amounts of residues GlcA-II, IV, VI, VII, and VIII in GXM 401 not determined.
[g] Not assigned.
[h] Assigned from 50 ms NOESY spectrum of respective isolate (from intraresidue H-1–H-5a cross peak).
[i] Not applicable.

spectrum of GXM 34. The corresponding H-1–H-2 and H-2–H-3, H-3–H-4 cross peaks for these residues are shown in Figs 6c and 6a, respectively. Residues GlcA-I (for which data are not shown) and GlcA-II (as shown in Figs 6a–c) lack the cross peaks indicative of Xyl residues; no distinct H-4–H-5 cross peaks are observable. Evidence that GlcA-I and GlcA-II are GlcA residues comes from the fact that these are the only residues giving strong intraresidue H-1–H-5 NOE cross peaks. Chemical shift assignments for Xyl and GlcA residues of the *O*-deacetylated GXM of isolates 298, 34, and 401 are presented in Table 2.

Portions of the 50 ms NOESY spectrum of GXM 298 are shown in Figs 7a and 7b. Aside from the two intraresidue GlcA H-1–H-5 NOE cross peaks marked (residues GlcA-I and GlcA-II, Fig. 7a) and the intraresidue Man H-1–H-2 cross peaks marked (Fig. 7b), all of the marked cross peaks are due to interresidue NOE cross peaks. In the

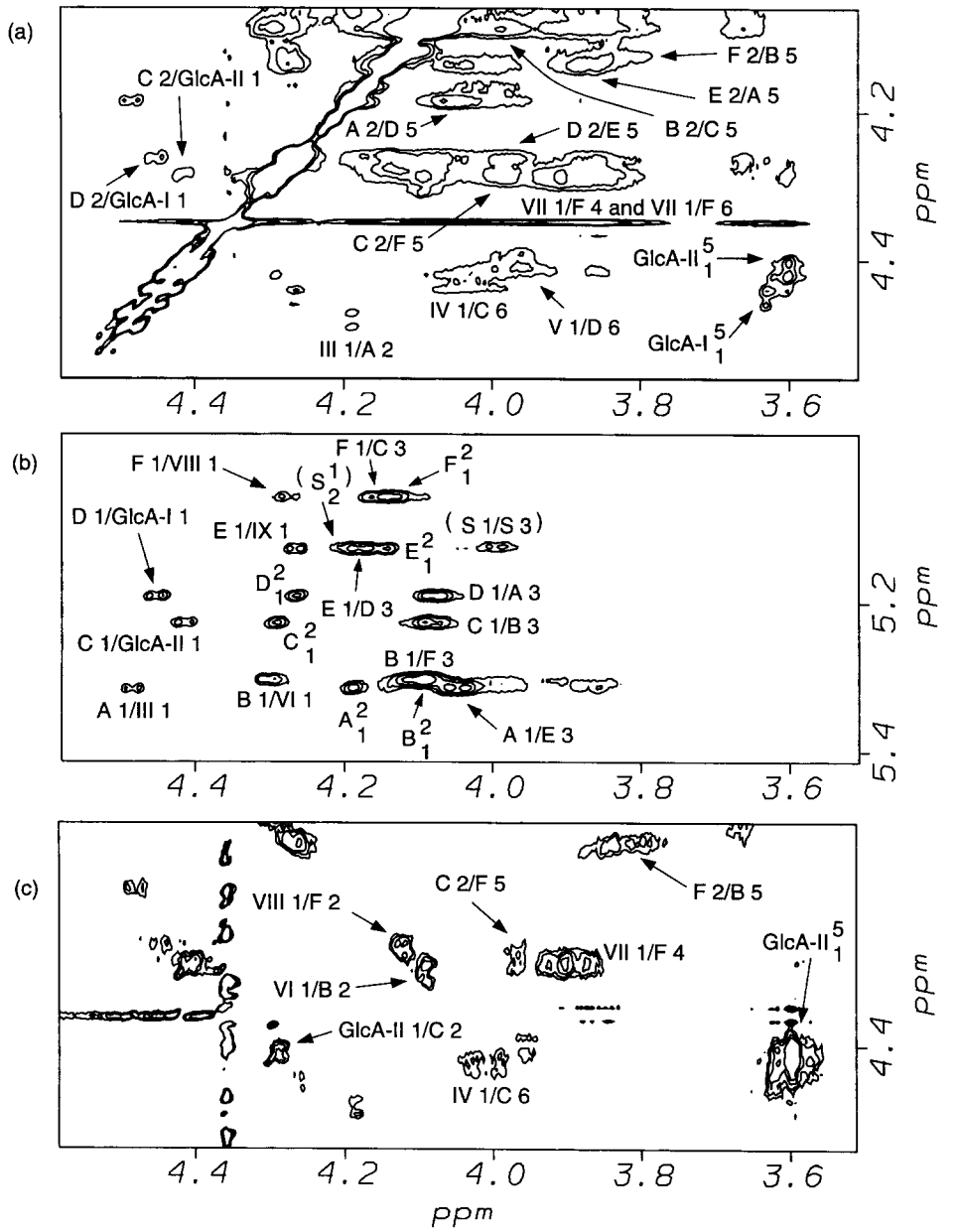

Fig. 7. (a) Part of the 50 ms NOESY spectrum of GXM 298. This region contains cross peaks due to through-space interactions of Xyl and GlcA H-1 protons (whose chemical shifts are found along the $F1$ dimension) with Man H-2, H-4, and H-6 protons (whose chemical shifts are found along the $F2$ dimension). Interresidue Man H-2–Man H-5 NOE cross peaks also appear in this region. (b) The region of the 50 ms NOESY spectrum of GXM 298 showing cross peaks involving Man H-1 protons (whose chemical shifts appear along the $F1$ dimension). The upper-case letters refer to Man residues, and the Roman numerals refer to Xyl and GlcA residues. The labeling for intraresidue NOE cross peaks is the same as for the DQF–COSY cross peaks in Figs 2, 3, and 5. Interresidue NOEs are marked as, for example, E 1/IX 1 to indicate through-space connectivity between Man-E H-1 ($F1$, or vertical axis) and Xyl-IX H-1 ($F2$, or horizontal axis). (c) Part of the 75 ms ROESY spectrum of GXM 34 showing approximately the same spectral region as (a). Only cross peaks involving residues of GXM octasaccharide **1** are marked in the manner described above. Only negative contour levels are shown.

5.3–5.0 ppm $F1$ region (corresponding to the H-1 chemical shifts of Man residues), each Man residue shows NOE cross peaks correlating H-1 with (1) H-3 of the Man residue to which it is (1 → 3) linked; and (2) H-1 of the Xyl or GlcA residue to which it is (1 → 2) linked. Additionally, Man H-2–Man H-5 interresidue NOE cross peaks (for instance, Man-B H-2–Man-C H-5) are shown in Fig. 7a for each (1 → 3) linkage showing a H-1–H-3 NOE cross peak in Fig. 7b (for instance, H-1 of Man-C to H-3 of Man-B). The β-Xyl-(1 → 2) (or GlcA) linkage also gives rise to interresidue Xyl (or GlcA) H-1–Man H-2 NOE cross peaks, some of which are obscured by unmarked intraresidue H-2–H-3 cross peaks in the 4.5–4.2 ppm $F1$ region shown in Fig. 7a. Interresidue NOE cross peaks between protons involved in β-Xyl-(1 → 4) linkages (IV H-1–C H-6, V H-1–D H-6, and VII H-1–F H-4) are also marked in this region. The VII H-1–F H-4 cross peak is unobscured in the 75 ms ROESY spectrum of GXM 34 (Fig. 7c).

The absence of intraresidue Man H-1–H-3 or H-1–H-5 NOE cross peaks confirms the α configuration for each Man residue. Based on the interresidue Man H-1–H-3 cross peaks, two GXM polymeric units are present in these serotype C isolates; these repeating structures consist of the backbone sequences (1) [→ 3)-α-Man-C-(1 → 3)-α-Man-B-(1 → 3)-α-Man-F-(1 →] and (2) [→ 3)-α-Man-D-(1 → 3)-α-Man-A-(1 → 3)-α-Man-E-(1 →]. Taking into account β-Xyl-(1 → 2), β-GlcA-(1 → 2), and β-Xyl-(1 → 4) linkages, these backbone sequences are present in octasaccharide **1** and heptasaccharide **2**.

4. Discussion

The *O*-deacetylated GXM of serotype C isolates 298, 34, and 401 have been found to contain differing amounts of octasaccharide **1** and heptasaccharide **2**. Despite the severe crowding of 2D NMR spectra, nearly complete assignment of proton signals has been achieved. Protons of Man, Xyl, and GlcA residues in **1** were largely assigned from the 2D NMR spectra of GXM 34; the same protons in **2** were largely assigned from spectra of GXM 401. Chemical shift assignments of **2**, the GXM structure long postulated for serotype B isolates [4,20], are consistent with those previously reported [28]. Proton chemical shift assignments of **1**, the GXM structure postulated for serotype C isolates [22,25], are reported for the first time.

With the nearly complete assignment of sugar residues, NOESY and/or ROESY spectra were used to sequence the residues. The linkages deduced are consistent with methylation analysis results that confirm the presence of trisubstituted Man residues (1-, 2-, and 3-linked), tetrasubstituted Man residues (1-, 2-, 3-, and 4-linked), and monosubstituted Xyl residues (1-linked) [23]. Linkages of the β-Xyl-(1 → 2) and β-GlcA-(1 → 2) residues were easily accomplished since NOE correlations are observed for a particular Xyl (or GlcA) H-1 to both H-1 and H-2 of the Man residue to which it is attached. α-Man-(1 → 3) linkages were obtained from the corresponding interresidue H-1–H-3 NOE cross peaks. Interresidue Man H-2–Man H-5 NOE cross peaks are also observed in Fig. 7a and are consistent with a $(\Phi,\Psi) = (-50°, -20°)$ conformation of an α-Man-(1 → 3) linkage [42]. From the NOESY spectrum of GXM isolate 298 shown in

Fig. 7b, the interresidue Man H-1–Man H-3 cross peaks as marked are consistent with the presence of structures **1** and **2** as either separate polymer chains or block structures. Since the chemical shifts of Man-A H-3 and Man-B H-3 are relatively close to one another, a switch of their assignments would result in spectral data consistent with **3**, a structure consistent with the approximately equal amounts of **1** and **2** in GXM 298. However, the presence of the interresidue NOE cross peaks Man-A H-2–Man-D H-5 and Man-B H-2–Man-C H-5 (labeled in Fig. 7a) confirm the α-Man-D-(1 → 3)-α-Man-A and α-Man-C-(1 → 3)-α-Man-A linkages present in **1** and **2**.

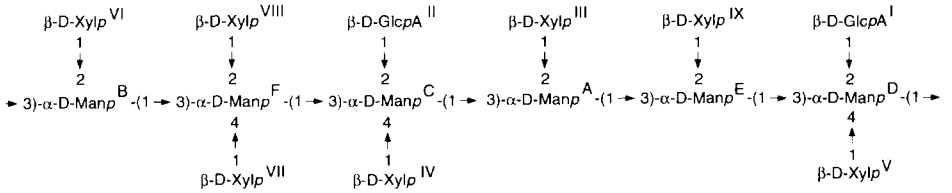

3

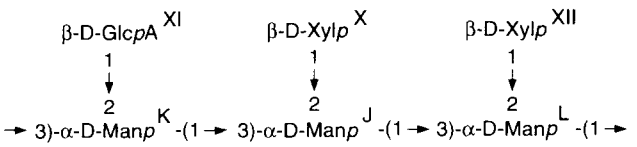

4

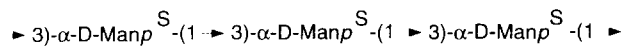

5

Whereas structure **1** is that usually shown in previously reported discussions of the GXM structure of serotype C isolates, the exact placement of the second β-Xyl-(1 → 4) residue (Xyl-VII as shown in **1**) has until now not been known. (Is Xyl VII linked to Man-F in **1**, or to Man-B?) Previous work [28] and an examination of molecular models show that a particular Xyl H-1 may show a stronger NOE to one of the Man H-6 protons (rather than to H-4) when a β-Xyl-(1 → 4) linkage is involved, so precise assignment of Man H-4 and H-6 protons is essential for correctly identifying NOE cross peaks involving the β-Xyl-(1 → 4) residues. These assignments were made for **1** using the DQF–COSY and TOCSY spectra of GXM 34.

A portion of the 75 ms ROESY spectrum of GXM 34 is shown in Fig. 7c; interresidue NOE peaks involving the β-Xyl-(1 → 4) residues of **1** (Xyl-IV and Xyl-VII) are marked. Based on the Man H-4, H-5, and H-6 assignments of residues Man-B, Man-C, and Man-F, it is clear that Xyl-IV is linked to Man-C. The marked Xyl-III NOE peak reflects NOE contacts to both Man-C H-4 and H-6, although H-6 is the stronger contributor to the overlapping cross peaks observed. The full width of the Xyl-VII NOE cross peak is consistent with an NOE contact to H-4 (and perhaps to H-6) of residue

Man-F. A hypothetical Xyl-VII H-1–Man-B H-6 NOE cross peak would be contained in the Xyl-VII cross peak observed, although the full width of the observed peak could not be explained in this case. There is, however, no indication of any NOE between Xyl-VII H-1 and Man-B H-4. Thus, the second β-Xyl-(1 → 4) linkage is to Man-F and not to Man-B.

The presence of at least one prominent minor Man resonance in *O*-deacetylated GXM 401 has been mentioned: Man-L, Fig. 1b. Inspection of the DQF–COSY spectrum of GXM 401 revealed numerous cross peaks not accounted for in structures **1** and **2** (Figs 2 and 8a). Most prominently, one extra Xyl or GlcA H-1–H-2 cross peak was observed in the DQF–COSY spectrum recorded at 68°C. A P.COSY spectrum of isolate 401 at 71°C revealed a second Xyl or GlcA H-1–H-2 cross peak that had been obscured by the HOD resonance at 68°C. These cross peaks are marked in Fig. 8a. A portion of a 75 ms ROESY spectrum of isolate 401 is shown in Fig. 8b. Along the $F1$ frequencies corresponding to the H-1 chemical shifts of Man-B and Man-C NOE, peaks not observed in the NOESY or ROESY spectra of isolates 34 or 298 may be seen: J 1–X 1, J 1–J 2, and J 1–L 3 at the Man-B H-1 chemical shift and K 1–GlcA-XI 1, K 1–K 2, and K 1–J 3 at the Man-C H-1 chemical shift. Faint NOE peaks are also observed for L 1–XII 1, L 1–L 2, and L 1–K 3 along the $F1$ axis corresponding to the chemical shift of Man-L H-1.

The chemical shifts of the extra protons labeled in Figs 2 and 8 are presented in Table 3. Since some of the DQF–COSY cross peaks expected for these protons in Fig. 2 were faintly visible (if not absent) or obscured by cross peaks involving protons of **1** or **2**, it was not possible to systematically delineate the spin systems of the Man-J, Man-K, Man-L, Xyl-X, GlcA-XI, and Xyl-XII residues for which chemical shifts are reported in Table 3, but the chemical shifts obtained agree with those found for hexasaccharide **4** from previous 2D NMR analyses of *O*-deacetylated GXM from serotype A isolates 201 [29] and 118 [40].

The presence of approximately equal amounts of octasaccharide **1** and hexasaccharide **4** in GXM 401 is now clear from the similar intensities of Man-L H-1 and Man-F H-1 resonances in Fig. 1b. Compared with heptasaccharide **2**, the extra Xyl in **1** offsets the lack of one Xyl in **4**; therefore previously reported analytical data for GXM 401 resemble those for a typical serotype B isolate [22]. Methylation analysis had indicated a small presence of 2,4,6-D-mannose for GXM isolates 298 and 401 [22]. This indicates the presence of a mannan structure as in **5**. The chemical shifts of Man residue Man-S, found in this work for isolates 298 and 34 and shown in Table 1, are consistent with mannan **5** on the basis of having observed similar resonances in previous work in this laboratory, not only from having observed small amounts of **5** in serotype A and D GXM, but also from having worked with mannan **5** itself. In addition, a S 1–S 3 NOE cross peak is present in the NOESY spectra of isolates 298 and 34 (as shown in Fig. 7b for isolate 298). It must be mentioned that a small amount of **5** is detectable in our NMR work since the resolution enhancement used to resolve the broad resonances of high-molecular-weight, highly substituted structures such as **1** favors detection of less rigid structures such as **5**.

The relative amounts of octasaccharide **1** in GXM isolates 34, 298, and 401 (approximately 75%, 50%, and 25%, respectively) are indicative of the quantitative

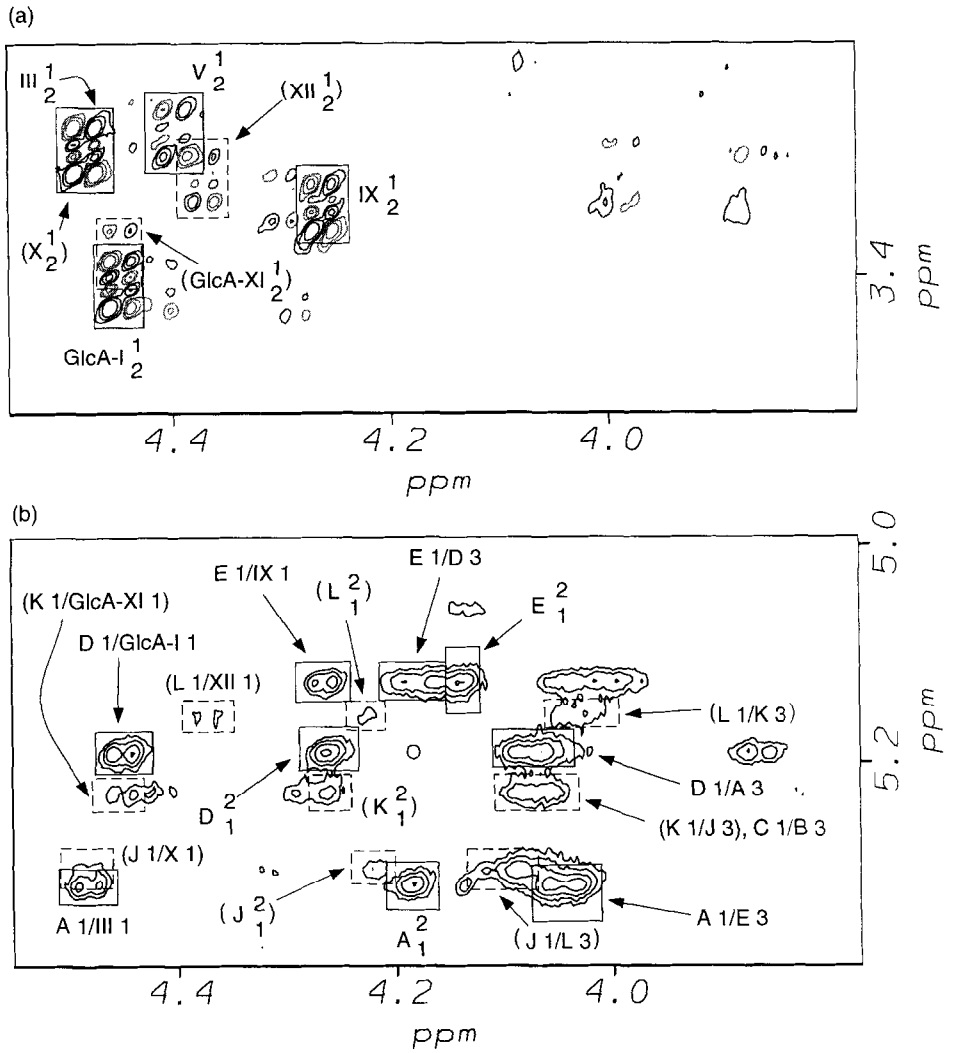

Fig. 8. (a) Portion of the phase-sensitive P.COSY spectrum of *O*-deacetylated GXM 401 recorded at 400 MHz and 71°C. H-1–H-2 cross peaks due to Xyl and GlcA residues of GXM heptasaccharide **2** are enclosed in solid lines; cross peaks due to Xyl and GlcA residues of GXM hexasaccharide **4** are boxed in dotted lines. Cross peaks due to residues of octasaccharide **1** are neither boxed nor labeled. (b) Part of the 75 ms ROESY spectrum (showing only negative contour levels) of the *O*-deacetylated capsular polysaccharide of isolate 401. The region shows NOE cross peaks involving Man H-1 protons (whose chemical shifts are found along the *F*1 dimension). As in (a), only cross peaks involving residues of **2** and **4** are boxed and labeled. Labeling is the same as for Fig. 7. The L 1–XII 1 cross peak was weak and had to be reproduced from a lower contour level of the data matrix.

differences in the serological activity of these strains with *C. neoformans* factor sera, as previously reported [26]. Having confirmed the presence of GXM heptasaccharide **2** (typical for serotype B isolates) in all three isolates and the presence of GXM

Table 3
^{1}H NMR chemical shifts of the ring protons of the constituent monosaccharides of **4**, as identified in the *O*-deacetylated GXM of *C. neoformans* serotype C isolate 401

	Chemical shift [a]					
	Man-J [b]	Man-K	Man-L	Xyl-X	GlcA-XI	Xyl-XII
H-1	5.293 [c]	5.223	5.153	4.480 [d]	4.448 [d]	4.372 [d]
H-2	4.217	4.259	4.221	3.286 [d]	3.380 [d]	3.309 [d]
H-3	4.065 [e]	4.033 [e]	4.082 [e]	n.a. [f]	n.a.	n.a.
H-4	3.810 [e]	3.836 [e]	3.686 [e]	n.a.	n.a.	n.a.
H-5a	n.a.	n.a.	4.030 [e]	n.a.	n.a.	n.a.
H-5e	– [g]	–	–	n.a.	n.a.	n.a.
H-6	n.a.	n.a.	n.a.	–	–	–

[a] In ppm relative to HOD as externally referenced according to temperature with DSS (δ 0.0) as internal standard.
[b] For residue labeling see formulae.
[c] Unless otherwise noted, chemical shifts were assigned from a ROESY spectrum recorded at 71°C and are reported with an accuracy of ± 0.003 ppm.
[d] Assigned from a P.COSY spectrum recorded at 71°C.
[e] Assigned from a DQF–COSY spectrum recorded at 68°C.
[f] Not assigned.
[g] Not applicable.

hexasaccharide **4** (typical for serotype A isolates) in isolate 401, we are now using 2D NMR to analyze intact, acetylated GXM isolates in order to determine how acetylation affects solution conformation and consequently serological activity. We hope to determine if variation in the disposition of the *O*-acetyl substituents in native GXM can explain why, for example, GXM 401 types as serotype C despite the presence of the minor portion of **4**. The assignments described herein are essential for the analysis of the ^{1}H NMR spectra of 6-*O*-acetylated GXMs.

The ^{1}H NMR assignments presented here are important for other aspects of the study of GXM from *C. neoformans*. Having assigned the proton NMR assignments for GXM from serotypes B [29] and D [28], we are completing proton NMR assignments of serotype A GXM. Using the H-1 signals of resolution-enhanced ^{1}H NMR spectra, in conjunction with the assignments herein reported for serotype C, we are selecting triads of mannose residues (such as **1**, **2**, and **4**) as the reporter of fine structure of GXM. Since we had not previously been able to detect the presence of minor structural GXM elements, such as **4** using ^{13}C NMR spectroscopy [23], the ^{13}C NMR assignments of mannose C-1 nuclei are not suitable for this purpose. A relational database for assigning the structure to any isolate of *C. neoformans* is being developed; in conjunction with the development of a neural network, it may be possible to serotype newly isolated GXM isolates from 1D ^{1}H NMR spectra.

Acknowledgement

This research was supported in part by Public Health Service grant AI-31769 from the National Institutes of Health.

References

[1] K.J. Kwon-Chung and J.E. Bennett, *Medical Mycology*, Lea and Febiger, Malvern, PA, 1992, pp 397–446.
[2] Zugar, E. Louie, R.S. Holtzman, M.S. Simberkoff, and J.J. Rahal, *Ann. Intern. Med.*, 104 (1986) 234–240.
[3] B.P. Currie and A. Casadevall, *Clin. Infect. Dis.*, 19 (1994) 1029–1033.
[4] R. Cherniak and J.B. Sundstrom, *Infect. Immun.*, 62 (1994) 1507–1512.
[5] A.K. Bhattacharjee, J.E. Bennett, and C.P.J. Glaudemans, *Rev. Infect. Dis.*, 6 (1984) 619–624.
[6] R. Cherniak, in M.R. McGuiness (Ed.), *Current Topics in Medical Mycology*, Springer-Verlag, New York, 1988, pp 40–54.
[7] S.H. Turner and R. Cherniak, in J.P. Latage and D. Boucias (Eds), *Fungal Cell Walls and Immune Response*, Springer-Verlag, New York, 1991, pp 123–142.
[8] R. Ikeda, T. Shinoda, Y. Fukazawa, and L. Kaufman, *J. Clin. Microbiol.*, 16 (1982) 22–29.
[9] D.E. Wilson, J.E. Bennett, and J.W. Bailey, *Proc. Soc. Exp. Biol. Med.*, 127 (1968) 820–823.
[10] J.E. Bennett, K.J. Kwon-Chung, and D.H. Howard, *Am. J. Epidemiol.*, 105 (1977) 582–586.
[11] J.E. Bennett, K.J. Kwon-Chung, and T.S. Theodore, *Sabouraudia*, 16 (1978) 167–174.
[12] K.J. Kwon-Chung, I. Polacheck, and J.E. Bennett, *J. Clin. Microbiol.*, 15 (1982) 535–537.
[13] R. Ikeda, A. Nishikawa, T. Shinoda, and Y. Fukazawa, *Microbiol. Immunol.*, 29 (1985) 981–991.
[14] K.J. Kwon-Chung, A. Varma, and D.H. Howard, in H. Vanden Bossche and D.W.R. Mackenzie (Eds), *Mycoses in AIDS Patients*, Plenum Press, New York, 1990, pp 103–113.
[15] M.N. Clancy, J. Fleischman, D.H. Howard, K.J. Kwon-Chung, and R.Y. Chimizu, *J. Infect. Dis.*, 161 (1990) 809.
[16] R. Rozenbaum, A.J.R. Goncalves, B. Wanke, and W. Vieira, *Mycopathologia*, 112 (1990) 33–34.
[17] G. St.-Germain, G. Noel, and K.J. Kwon-Chung, *Eur. J. Clin. Microbiol. Infect. Dis.*, 7 (1988) 587–588.
[18] J.J. Muyembe Tamfum, D. Mupapa Kibadi, L. Nganda, D. Mgwala Bikindu, T. Kuezina, I. Kela We, and J. Vandepitte, *Med. Trop. Mars.*, 52 (1992) 435–438.
[19] W. Peetermans, H. Babbaers, J. Verhaegen, and J. Vandepitte, *Acta Clin. Belg.*, 48 (1993) 405–409.
[20] D.K. Henderson, J.E. Edwards, Jr, W.E. Dismukes, and J.E. Bennett, *Abstr. Annu. Meet. Am. Soc. Microbiol.*, 1981, p 315, abstr F-11.
[21] S.H. Turner and R. Cherniak, *Carbohydr. Res.*, 211 (1991) 103–116.
[22] R. Cherniak, L.C. Morris, and S.H. Turner, *Carbohydr. Res.*, 223 (1992) 263–269.
[23] R. Cherniak. L.C. Morris, and S.A. Meyer, *Carbohydr. Res.*, 225 (1992) 331–337.
[24] S.H. Turner, R. Cherniak, E. Reiss, and K.J. Kwon-Chung, *Carbohydr. Res.*, 233 (1992) 205–218.
[25] A.K. Bhattacharjee, K.J. Kwon-Chung, and C.P.J. Glaudemans, *Immunochemistry*, 15 (1978) 673–679.
[26] A.K. Bhattacharjee, K.J. Kwon-Chung, and C.P.J. Glaudemans, *Mol. Immunol.*, 16 (1978) 531–532.
[27] T. Belay, R. Cherniak, and T. Shinoda, *Infect. Immun.*, 61 (1993) 2879–2885.
[28] M.A. Skelton, R. Cherniak, L. Poppe, and H. van Halbeek, *Magn. Reson. Chem.*, 29 (1991) 786–793.
[29] M.A. Skelton, H. van Halbeek, and R. Cherniak, *Carbohydr. Res.*, 221 (1991) 259–268.
[30] M.A. Skelton, *Two-Dimensional N.M.R. Spectroscopic Investigations of the Polysaccharide Antigens of Cryptococcus neoformans*, Thesis, 1991, pp 48–66.
[31] J. Dabrowski, in W.R. Croasmun and R.M.K. Carlson (Eds), *Two-Dimensional NMR Spectroscopy. Applications for Chemists and Biochemists*, VCH, New York, 1994, pp 741–783.
[32] D.J. States, R.A. Haberkorn, and D.J. Ruben, *J. Magn. Reson.*, 48 (1982) 286–292.
[33] D. Neuhaus, G. Wagner, M. Vasak, J.H.R. Kagi, and K. Wuthrich, *Eur. J. Biochem.*, 151 (1985) 257–273.
[34] M. Rance, O.W. Sorensen, G. Bodenhausen, G. Wagner, R.R. Ernst, and K. Wuthrich, *Biochem. Biophys. Res. Commun.*, 117 (1983) 479–485.
[35] A. Bax and D.G. Davis, *J. Magn. Reson.*, 65 (1985) 355–360.
[36] J. Jeener, B.H. Meier, P. Bachmann, and R.R. Ernst, *J. Chem. Phys.*, 71 (1979) 4546–4553.
[37] A. Bax and D.G. Davis, *J. Magn. Reson.*, 63 (1985) 207–213.
[38] A.A. Bothner-By, R.L. Stephens, J.-M. Lee, C.D. Warren, and R.W. Jeanloz, *J. Am. Chem. Soc.*, 106 (1984) 811–813.

[39] H. Kessler, C. Griesinger, R. Kerssebaum, K. Wagner, and R.R. Ernst, *J. Am. Chem. Soc.*, 109 (1987) 607–609.
[40] D. Marion and A.J. Bax, *J. Magn. Reson.*, 80 (1988) 528–533.
[41] B.E. Bacon and R. Cherniak, unpublished results.
[42] P. de Waard, B.R. Leeflang, J.F.G. Vliegenthart, R. Boelens, G.W. Vuister, and R. Kaptein, *J. Biomol. NMR*, 2 (1992) 211–226.